Original scientific paper

LIGHTENING STRUCTURES BY METAL REPLACEMENT: FROM TRADITIONAL GYM EQUIPMENT TO AN ADVANCED FIBER-REINFORCED COMPOSITE EXOSKELETON

Cristiano Fragassa

Department of Industrial Engineering, Alma Mater Studiorum University of Bologna, Italy

Abstract. *A redesign procedure used for introducing new functional properties in innovative gym equipment is here reported. It is based on a metal replacement action where a tempered steel was firstly replaced by an aluminum alloy and then by high strength-to-weight fiber-reinforced polymers. The effect of fiber properties (as strength and volume ratio) and plies stacking sequences (as thicknesses and orientation) were investigated. Numerical analyses, done by Ansys ACP, allowed evaluating the stress-strain behavior in realistic boundaries and quasi-static loads, comparing materials and layouts in terms of stiffness. The single-layered shell method with additional integration points was preferred as a technique for discretizing composite laminates. Maximum Principal Stress and Maximum Distortion Energy (Tsai-Hill) were applied as anisotropic failure criteria. Changes in geometry were also considered given their relevant effects on parts and processes. Specifically, this paper is focused on a representative component of the main kinematic chain (the 'forearm') and details the different redesign phases for that part. The chosen solution consisted of 14 layers of unidirectional and bidirectional carbon fiber-reinforced pre-pregs, offering a 68 % weight reduction with respect to a solid aluminum component with equal stiffness. The part was manufactured by hand lay-up and cured in autoclave. This redesign practice was extended to the rest of the equipment allowing its transformation into an exoskeleton.*

Key Words: *Material Design, Functional Design, Exoskeleton, Fiber Reinforced Polymers, Strength-to-weight Ratio, Exercise Machine, Rehabilitation*

1. INTRODUCTION

The replacement of metals by polymer-based materials has become a common practice nowadays in many engineering areas due to a series of benefits, both in terms of the components and processes they are able to provide.

These materials offer the possibility of conducting a thorough system optimization based on weight reduction and performance increase based on a tailored-design premise. Designers can also count on thermal stability, resistance to corrosion and oxidation, thermal, acoustic, and electrical insulations through shorter manufacturing processes and reduced material waste, thus increasing overall savings [1].

Automotive and aircraft industries were the first industrial sectors to benefit from a progressive metal replacement. A gradual decrease of ferrous (as steel alloy, carbon steel, cast iron and wrought iron) and non-ferrous metals (primarily aluminum) presence in the vehicle design over the years is reported [2]. In these cases, metallic alloys are often replaced by high performance polymers and reinforced polymer sandwiches on the way to improving the parts performance. A representative case is stated in [3] in which reinforced plastic replaced steel achieved 23% of weight reduction in the passenger airbag housing. This new component also successfully passed all the strict validation tests.

However, each major industrial sector has been involved in replacing, to some extent, metals with plastic polymers [4]. According to their lower material density, a 20/30% weight reduction can be generically estimated in relation to their use, even more in the presence of high strength-to-weight fiber-reinforced polymers (FRP) [4, 5].

Therefore, the material replacement has become such a common and effective design strategy that some cases emerge in which designers have even replaced composites with composites despite trying to (re)introduce metals. This situation is evident, for instance, in a work concerning railway sleepers [6]. They were traditionally made by hardwood timbers and the use of metal (carbon steel) or concrete was under evaluation. Extending the material alternatives to composites as well, the best solution in terms of strengthening and in-service costs reduction responded to the utilization of fiber (glass or carbon) reinforced composites, either as a single constituent material, or as timber reinforcement layers (*e.g.* applied by wrapping).

At a glance, comparing a quite common carbon fiber-reinforced polymer (CFRP) as *Toray T700*, a structural aluminum alloy as 6061-T6 (Al) and a conventional tempered steel as ISO C40, it is easy to notice the potential benefits offered by CFRP regarding the combination of lightness and stiffness. The CFRP specific weight (2200 kg/m^3) is 20% lower than the mentioned lightweight Al alloy (2720 kg/m^3) and 3.5 times lighter than SST (7800 kg/m^3). At the same time, the CFRP mechanical properties are also remarkable [7] with Young's modulus (*E*) up to 112 GPa, and Ultimate Tensile Strength (*UTM*) up to 1100 MPa), making this material a consistent alternative to both Al (71 GPa and 310 MPa) or SST (190 GPa, 510 MPa) in many structural applications [7].

Moreover, the variability due to anisotropy (e.g. *E* and *UTM* ranging between 35-112 and 0.25-1.1 GPa, respectively, for *T700*) permits optimizing part geometries based on local stress distributions [8]. For instance, in [9] a genetic algorithm was used during the process of design optimization ('layout design') of 8-layer composite laminates intended to withstand transverse or in-plane loads. Aspects such as fiber type (*i.e.* glass, carbon, and aramid), ply orientation and thickness were modified following a multi-objective

approach while Finite Elements (*FEs*) permitted verifying failure criteria (*i.e.* by means of the Tsai–Wu theory). Depending on the specific design target, the algorithm permitted to widely range out in terms of weight ($\pm 33\%$), deflection ($\pm 76\%$) and cost ($\pm 43\%$).

However, the design concept that material changes can improve product performances is fairly known among designers. Less frequent is the case in which a metal replacement leads to significant changes in the product functionality such as it is reported hereby.

This paper proposes the case of advanced gym equipment, innovative with respect to several functional solutions, and that is able to offer a rather exclusive gym training method. The equipment is lightened thanks to a combination of geometric modifications and metal replacements - from steel to aluminum and, finally, to reinforced composites – on the way to being transformed into a wearable exoskeleton, thus incorporating new functionalities.

Composite exoskeletons, using carbon or analogue extra-light fibers as reinforcement, are available nowadays, although not very popular, especially pondering costs. In most cases they are powered by external systems like electric motors, pneumatics, levers or hydraulics allowing movements with increased strength and endurance. Applications include but are not limited to military, airspace, advanced industry (in the presence of heavy loads), civilian (firefighters and rescue workers) and medical applications.

The first exoskeleton was probably developed in 1972 in Serbia as a medical device for rehabilitation of paraplegics [10]. It was active unwearable equipment, made by rather traditional materials and design solutions. Then, a long time passed before the next exoskeleton that rose to prominence was developed in the US in 1985 as a powered suit of armor [11]. Since then, interest in exoskeletons has been growing year after year and numerous studies describe their design techniques [12-15], including a special attention to an optimal material selection. For instance, the case of a passive/active exoskeleton for index finger rehabilitation is reported in [16]. This article, where much attention is paid to assuring the highest precision of movements, highlights how the correct definition of allowed trajectories (and, therefore, of kinematic joints) represents one among the most challenging aspects in the exoskeletons design.

A study of the state-of-the-art in this field identified several exoskeletons that inspired the present development. In particular, in [17] a wearable structure having links and joints corresponding to a human upper body was patented. Similar design assumptions were adopted for choosing and positioning connecting elements that enabled controlling the system movements. Additional technical specifications, originating from [17], were used here for the design of gym equipment, even if this prototype was conceived as a non-wearable machine at that time.

In line with the mentioned literature review, the current study demonstrates how the redesign procedure of a metallic structure into a fiber-reinforced composite one allowed a significant reduction in weight. Therefore, the heavy supporting frame turned out to be unnecessary, transforming the equipment into an exoskeleton and adding new functions.

To the best knowledge of the author, this is the first exoskeleton designed to ensure: 1) a completely free/unconstrained movement of the upper body, and 2) a constant and 'fluid' resistance, related to the speed of the movement but independent of location and direction. In addition, this exoskeleton was also designed to be active, thanks to the progressive replacement of the traditional frictional elements with magnetorheological torque transmission devices, already investigated in a previous work [18].

2. GEOMETRY AND DESIGN

2.1 Equipment

A gym exercise machine typically creates an opposition load to be overcome as
1. *Gravity force*: the load is constant, generated by the weight of an object (as handlebar, barbell, *etc.*), often driven and/or constrained by a mechanism.
2. *Elastic force*: the load is proportional for intensity to the displacement, generated according to the spring principle (elastic bands, *etc.*).
3. *Isokinetic force*: the load depends on the speed, increasing along with the relative speed induced on a mechanism (*e.g.* friction dumpers).
4. *Pneumatic / hydraulic force*: the load is generated using active mechanisms that also define every aspect of the movements (as hydraulic or pneumatic pistons)

All these forces are generally constrained according to two main schemes:
a. *free configuration*, where forces are directed according to a single direction as, *e.g.*, the weight force always downwards; the elastic force with direction along the anchor point; the isokinetic one according to the direction of cables and wires.
b. *structured configuration*, where forces are guided by means of articulated mechanisms.

With respect to these concepts, the gym machine under investigation was fully designed to be alternative and innovative. It can reproduce the complex kinematics and dynamics of the upper limbs in accordance with the following postulates:
1. *Ergonomics*: the structure must adapt according to the person's build. The functional elements of training must support the user's motor skills.
2. *Functionality*: the work paths, as well as the positions must be chosen as much as possible by the user and not set by the machine. Setting too many constraints penalizes the user's abilities in expressing primary and consequently healthy skills.
3. *Force*: the force of opposition to the movement must exclude the effect of gravity (weight force), the variation of intensity according to the arc of action (elastic force) and the dependence on the speed of execution (isokinetic force). The load distribution must be intrinsic to the instrument and be activated in a resistant form only during its use.

The result is necessarily an anthropomorphic structure, dressed on the user (Fig. 1).

In particular, by means of a vest the athlete wears the system and interacts with it through independent articulated segments. Thus, the functionality of the human structure has been resumed, supporting it in its mechanical complexity.

Main elements are:
-   ***base***: a fixed base and frame, resting on the ground and supporting moving parts;
-   ***jacket***: a movable system, to be fixed with straps, used for height adjustment and tutoring during the user's vertical movements;
-   ***trapezoids***: a movable mechanism, able to replicate the shoulder movements;
-   ***segments***: a cinematic chain, able to replicate the upper limb movements. Each side includes three segments, staying for ***arm***, ***forearm*** and ***hand***, integrated by resistive elements. The *hand* also includes a ***handle*** representing the element of interaction with the athlete and integrating the resistance management consoles.

These elements are shown in Table 1 together with a prediction of parts' weight done in accordance with geometry and specific weights. These values can be considered as a plausible estimate of the 'best attainable weight' that the different parts could have if made of metal. An attention was also paid to consider the proper manufacturing processes: sheet metal working (for steel) and tool machining (for steel or aluminum). Accessory elements (such as resistors and joints) were also incorporated as weight.
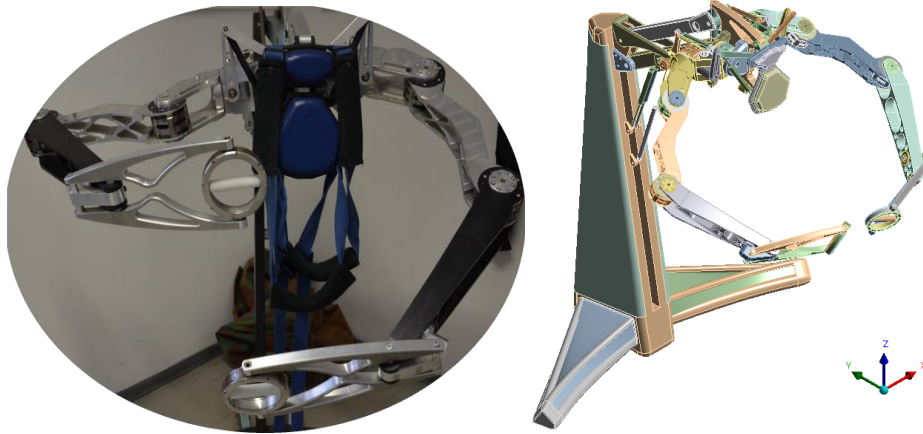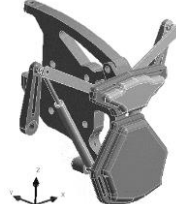

Fig. 1 The innovative gym equipment (metal version): it allows free movements in space offering a reaction of constant intensity

Table 1 Main parts of the gym equipment and weight estimation

Base	Trapezoids	Jacket	Segments
Steel	Aluminum	Aluminum	Aluminum
155 kg	21 kg	10 kg	17 kg

The first prototype was developed, assembled, and applied for functional tests. Wherever convenient, tempered steel, very common in the case of gym machines, was preferred with the scope to speed up construction and reduce costs. In particular, the large basement was (simplified and) made by metal sheet. Many of the remaining parts were made by CNC machining. An aluminum alloy was also used with the scope of lightening.

After a six-month testing period in operational environment (a gym), it was possible to confirm the main design choices and functionalities. Nevertheless, also evident was the opportunity to move towards further improvements.

The current work starts from this condition and, in particular, from the demand of making the entire structure lighter and leaner. Such an opportunity goes beyond the usual reasons and deeply affects the machine functionality.

The equipment, as mentioned, works by offering a free movement in space coupled with a constant reaction. This objective is achieved by combining two main effects: 1) elements always balanced and in equilibrium (with respect to any spatial configuration of the equipment); 2) constant resistance concentrated in specific elements, placed at the level of the joints. However, during the movements a further factor emerges: 3) the inertial force, opposed to the motion and proportional in intensity to the speed changes. Due to the high inertial masses involved, a general complication in using the equipment was noted for the period of tests, especially during the initial movements.

2.2 Design changes

The redesign process followed two routes: design changes in shape and in materials. However, the article is limited on those geometric changes strictly related to a proper exploitation of materials (ignoring when they simply aimed at reducing volumes). In addition, in order to simplify the description, it limits the narrative to a single component of the kinematic chain (the 'forearm'), but reports results with respect to the entire machine.

Specifically, the design work started with a *tempered steel* component (the 'forearm') and then went through its evolution in *aluminum alloy* and ended up with the final version in *reinforced composite*.

Table 2 reports this design progress showing changes in shape and in weight. Weights were estimated considering geometry and specific weight. Manufacturing technology are also listed (*i.e.* tool machining for steel, die casting for aluminum and hand lay-up with autoclave molding for composites). Table 3 specifies the main material properties related to the chosen materials [19, 20]. In the case of the composite, properties and weight are here indicative before an optimization based on the definition of proper stratifications.

Shape changes were introduced to favor the lightening, but also to meet some aspects regarding the different manufacturing processes. Specifically, it can be noted that the steel version (A) was made by CNC machine tool in two solid pieces. It represented the proper solution for prototyping the first machine to be functionally tested in gym.

Table 2 Design evolution

Steel	Aluminum	Composite
Tool Machining	Die Casting	Autoclave
4.4 kg	1.0 kg	~0.5 kg

Table 3 Comparing different versions [19, 20]

Version		A	B	C
Material		Steel	Aluminum	Composite
Type		C40	6061-T6	T1000
Young Modulus (*E*)	GPa	193	71	121
Ultimate Strength (*UTS*)	MPa	586	460	2231
Yield Strength *(YS)*	MPa	207	250	-
Poisson Ratio	-	0.31	0.33	0.27
Density	kg/m^3	7850	2770	1490

The aluminum version (B) was designed to make the whole machine and its parts lighter. It was planned to be manufactured in die-casting. It was made as a 1:5 scale model using rapid prototyping techniques, but never manufactured in true scale, because it was overtaken by the composite version (C).

However, aluminum die-casting offered a broader range of shapes in comparison to steel machining. It allowed the 'forearm' to be shaped in the way to reduce it to a single part (instead of two). Non-essential areas in terms of function or resistance were also removed thanks to the proper definition of shapes.

In addition, an excellent aluminum was selected, the 6061-T6, a lightweight and high-resistant structural material that can be further strengthened through alloying and heat treatments. Among others, its advantages are low density, high strength-to-weight ratio, good corrosion resistance, ease of fabrication and diversity of form. This first material change achieved a preliminary weight reduction (from 4.4 to 1.0 kg) to be decreased over by using fiber-reinforced plastics.

Starting with this update (B), several changes in geometry were introduced as well with the scope of considering the composite manufacturing technology. Specifically, as said, autoclave molding was preferred: thanks to high temperatures and pressures, it allows the production of composite parts characterized by high concentration of reinforcing fibers. Therefore, several changes had to be introduced with respect to this geometry, as shown in Fig. 2.
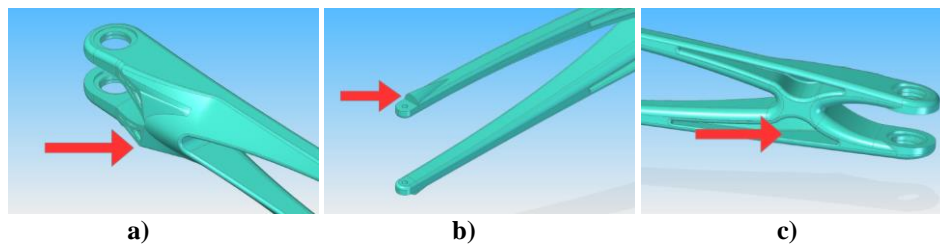

| a) | b) | c) |

Fig. 2 Shape changes in the case of composite version by eliminating the: a) undercut; b) shim; c) lightening notches (version B, in aluminum, is shown)

The aim of the changes is to simplify mold productions and parts extraction, such as:
a. Elimination of the upper undercut. The undercut is in the form of the fins, arranged in the top of the segment. Niches are also present, acting as containment tank for any glue overflow during parts' assembly.

b. Elimination of the shim positioned on the terminal. Its thickness has the purpose of optimizing the ergonomic appearance. In fact, this area hosts the handle, the element of interaction with the hand of the user.
c. Elimination of the lightening notches. Cut-outs are provided for lightening the part and for driving forces in conditions of flexural-torsional loads.

All these design measures, used to reinforce the aluminum component in specific areas, can be replaced by an appropriate layering in the case of composites.

3. MATERIALS AND METHODS

3.1 Fiber reinforced thermoplastics

Two high strength-to-weight ratio composites were used, reinforced by *T800* and *T1000* carbon fibers. Manufactured by *Toray Composites Materials Inc*, they are among the strongest fibers (230 GPa) available on the market. The real difference between them is therefore mainly linked to the fact that a unidirectional (*UD*) weave was chosen for the T1000 while the T800 was bidirectional (*BD*).

These fibers were supplied in the form of pre-impregnated fabrics *(Prepreg)* on *Epoxy*. Epoxy produces a strong and stiff structure with good adhesion to the carbon fibers. The fabrics, manufactured in rolls, already contain an optimized balance of epoxy resin and carbon fiber. The low resin-to-carbon ratio accentuates the ability of the carbon fibers on the way to minimizing weight and maximizing properties. In the specific case, T1000 and T800 were able to guarantee the maximum optimization of the fiber content which usually achieves 60% (after curing).

CFRP are shown in Table 4 in which a marked anisotropy is also evident.

Table 4 Main material properties for Epoxy Prepreg, Carbon (230 GPa) [20]

Material	Unit	T1000	T800
Type		UD	BD
Fiber		Carbon (230GPa)	Carbon (230GPa)
Matrix		Epoxy	Epoxy
Form		Prepreg	Prepreg
Thickness	mm	4x0.15	0.30
Properties			
Density	Kg/m^3	1490	1420
Young's Modulus $(E)^*$	MPa	121000, 8600, 8600	61340, 61340, 6900
Shear Modulus $(G)^{**}$	MPa	4700, 3100, 4700	19500, 2700, 2700
Poisson's Ratio $(v)^{**}$	-	0.27, 0.40, 0.27	0.04, 0.30, 0.30
Stress limits			
Tensile $(UTS)^*$	MPa	2231, 29, 29	805, 805, 50
Shear**	MPa	60, 32, 60	125,65,65
Strain limits			
Tensile Strength*	%	1.67, 0.32, 0.32	1.26, 1.26, 0.80
Shear Stress Limit**	%	1.2, 1.1, 1.2	2.2, 1.9, 1.9

along *(x, y, z) **(xy, yz, xz)

UD and BD prepregs were provided with 0.15 and 0.30 mm of thicknesses, respectively. However, very thin UD fabrics were always used by overlapping 4 layers (therefore, in the following section, a UD_{x4} layer means a 0.6 mm stratification of T1000, made by overlapping 4 layers of 0.15mm keeping the fibers along the same directions).

Ansys Workbench 19.3 platform was used for performing the numerical analysis. As material models, the *Ansys* internal library was exploited, selecting "*Epoxy Carbon UD (230 GPa) Prepreg*" and "*Epoxy Carbon Woven (230 GPa) Prepreg*" for T1000 and T800 respectively where default properties were changed in accordance with Table 4.

3.2 Stacking sequences

Ansys ACP toolkit was also permitted to build exact layouts. Specifically, the composite layout was recreated by defining the series of overlapping fabrics and their orientation, both reciprocal and with respect to the component. *ACP* allows us to do this, by identifying the specific stratification, layer by layer, orientation by orientation, with respect to each zone.

Ten different layouts (namely *L1, L2, ..., L10*) were defined and applied. They are detailed in Table 5 where material and orientation are reported per each layer. In the case of the *L6-L10*, a symmetrical doubling of the stratification has to be considered.

Table 5 Composite layouts

		L1		L2		L3		L4		L5	
	1	BD	0/90	BD	0/90	BD	0/90	BD	±45	BD	±45
	2	BD	±45	UD_{x4}	±45	UD_{x4}	0	UD_{x4}	0	UD_{x4}	0
	3	BD	±45	BD	0/90	BD	0/90	BD	±45	UD_{x4}	0
	4	BD	0/90							BD	±45
Layers		4		6		6		6		10	
Thickness *(mm)*		1.2		1.2		1.2		1.8		1.2	
Weight *(g/m²)*		1.70		1.75		1.75		1.75		2.64	

		L6		L7		L8		L9		L10	
	1	BD	0/90	BD	0/90	BD	0/90	BD	0/90	BD	0/90
	2	UD_{x4}	0	UD_{x4}	0	UD_{x4}	0	BD	±45	UD_{x4}	0
	3	BD	0/90	BD	±45	BD	±45	UD_{x4}	0	BD	±45
	4	*~ symmetry ~*		BD	±45	BD	0/90	BD	±45	UD_{x4}	0
	5			*~ symmetry ~*		*~ symmetry ~*		BD	0/90	BD	±45
	6							*~ symmetry ~*		*~ symmetry ~*	
Layers		*12*		*14*		14		16		22	
Thickness *(mm)*		2.4		3.0		3.0		3.6		4.2	
Weight *(g/m²)*		3.49		4.34		4.34		5.20		6.32	

The laminates were made by overlapping up to 22 layers of UD fabrics, at an orientation of 0° (occasionally 45° and -45°), and BD fabrics, at 0°/90° or ±45°. Between these configurations, only the first two (*L1* and *L2*) were quasi-isotropic (*i.e.* with in-plane isotropic properties). All the others are anisotropic, better responding to the particular physical configuration (geometry, loads, constrains) under examination.

Thickness varies from 1.2 (*L1*) to 4.2 mm (*L10*) with a specific weight slightly changing between 1420 and 1467 kg/m^3. However, layouts can be better compared using the weight per unit area, usually expressed in g/m^2: it varies between 1700 and 6320 g/m^2 for a thickness of, respectively, 1.2 (*L1*) and 4.2 mm (*L10*). As reference, a 4.2 mm aluminum foil in 6061-T6 has a weight of 11.6 kg/m^2.

3.3 Loads and Constrains

The comparison was made through numerical analysis in static load configuration. The load value was considered equal to 750N: the real value of the applied force depends on various parameters (*e.g.* resistances, inertia masses), but a maximum effort of 750 N on each of the handles was considered adequate to represent a proper load for the proposed use (*i.e.* exercises in gyms).

According to the so-called *human engineering*, the study of people in their working environment in order to maximize safety or efficiency, this value represents the maximum horizontal push forces exertable intermittently and for short periods of time in the case of male personnel [21]. Actually, this load is considered as representative when applied on the back, if braced against a vertical wall and feet anchored on a perfectly nonslip ground. In the case of push and pull, this load is reduced to 500 N when applied on both hands (or one shoulder) and 250 N on one hand.

The applied constraints are similar to those expected in the real kinematic chain. In particular, there is a clear difference between version A, with a double constraint (double fixed support), and versions B and C with a single constraint (single fixed support), as in Fig. 3. This makes the new configurations more critical in terms of stresses and strains.
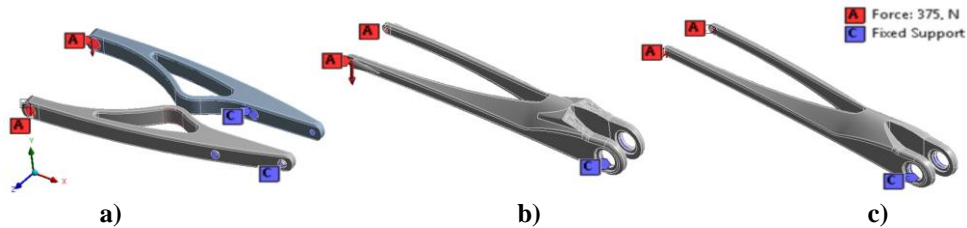

Fig. 3 Loads and constrains applied to: a) steel; b) aluminum and c) composite parts
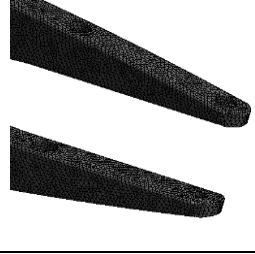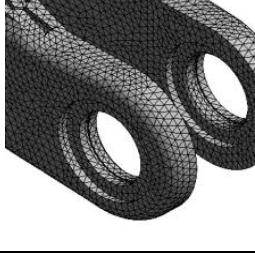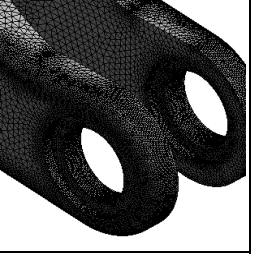
3.4 Numerical Discretization

Meshing was done using *3D ten-noded tetrahedral* elements (*Tet10*) in the case of steel (version A) and aluminum (version B), and *2D three-noded triangular* elements (*Tri3*) in the case of CFRP [22]. Finite Element (maximum) dimension was kept equal to 2.5mm. Details are available in Table 6. A control on the deformation energy of FEs is allowed to verify the absence of critical situations in the mesh (*e.g.* 'hourglass effect').

The so-called *single-layer shell method* was used for discretizing the composite layout. This simplification, quite common in the presence of geometrically complex structures, permits us to investigate the phenomena at the level of macroscale. With a proper conversion in properties, it reduces a multilayered laminate to an equivalent single

layer laminate with shell elements all along the surface and integration points (IP) throughout the thickness [22, 23].

Table 6 Numerical discretization by Finite Elements (FEs)

Finite Elements			
Denomination	*TET10*	*TET10*	*TRI3*
Type	Solid	Solid	Shell
Description	*10-noded tetrahedral*	*10-noded tetrahedral*	*3-noded triangle*
Dimension	2.5 mm	2.5 mm	2.5 mm
Elements *(tot)*	678 235	217 601	166 756
Nodes *(tot)*	970 550	324 752	83 372

Specifically, an IP was set per each layer (*i.e.* without additional IP for investigating the interfaces between layers). In such a way it was possible to limit the number of FE speeding up the simulation focusing the attention on in-plane phenomena [22, 23]. However, this methodological limit has no practical effect on the present study.

4. RESULTS AND DISCUSSION

4.1 Aluminum vs. Steel

Fig. 4 shows the results of the simulations performed on the part, in steel (version A) and aluminum (version B) expressed as (equivalent Von-Mises) stresses and displacements. The values are quite different in the two cases, due to differences in: a) geometry; b) material; c) constraint. The maximum stress reached in the components is very far from the critical conditions of failure (UTS) or yield (YS).

In particular, maximum stress values of 58.9 and 99.7 MPa are evident for steel and aluminum, much lower than 586 and 460 MPa as UTS (or 207 and 250 MPa as YS).

Thus, it is possible to say both these components work with safety coefficients higher than 2.5 making convenient to prefer the aluminum solution (version B).

This version, in fact, besides being 4 times lighter, also present other advantages such as: a) reduced overall dimensions; b) a single fixing point; c) better exploitation of material properties with stress fields more widely distributed; d) use of a production technology suitable to produce large numbers; e) aesthetics and ergonomics. On the other hand, the higher displacement (3.8 vs. 1.3 mm) of aluminum does not generate dysfunctions.
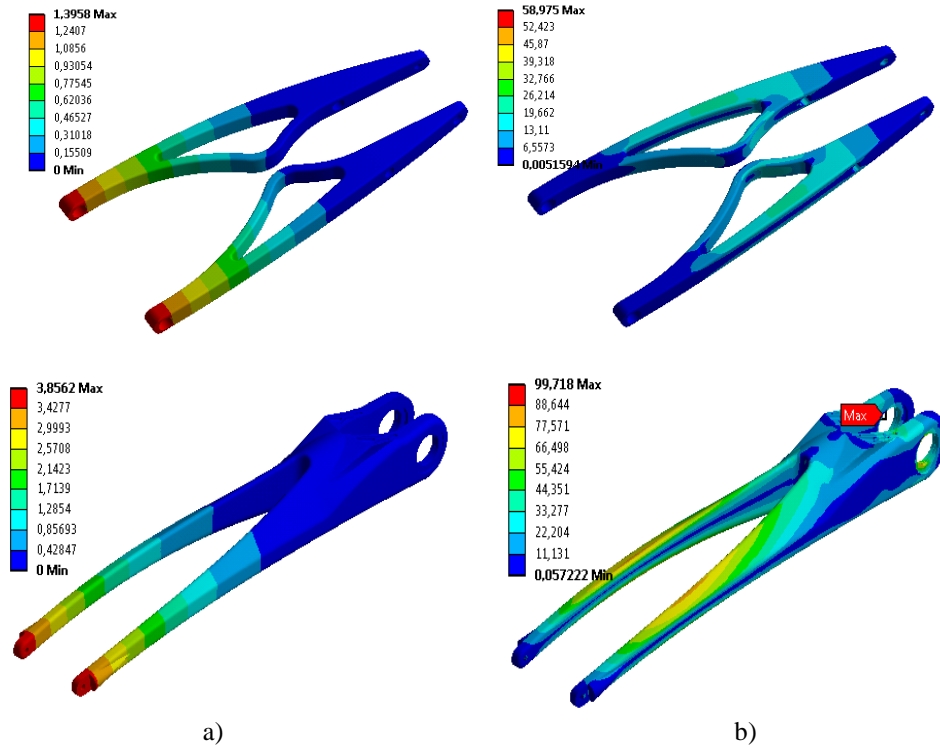
a)   b)

Fig. 4 Comparing steel (up) and aluminum (down) parts in terms of: a) displacements (in mm); b) Equivalent Von Mises stress (in MPa)

4.1 Composite vs. Aluminum

As the next step, different composite layouts were modeled by numerical analysis and compared with aluminum in terms of stiffness (Tab. 5).

The first objective was to identify an initial stratification, able to ensure a maximum displacement for the composite part (version C) similar to the aluminum one (version B) despite of a lower weight in the case of composite.

At this point, preliminary verified was also the presence of appropriate conditions on the stress distribution, far from the material limit values. For this purpose, the maximum principal stress (MPS) in the most stressed layer was compared with the *T800* (BD) tensile stress limit (UTS), equal to 805 MPa. A better check on failure criteria was postponed to the final configuration.

In particular, 10 layouts were considered, as displayed in Fig. 5, where a progressive reduction of displacement is evident as the laminate complexity increases. The graph also clarifies the advantage offered by the composites with respect to metals in terms of weight. In each case, compliance with the resistance conditions is also assured.
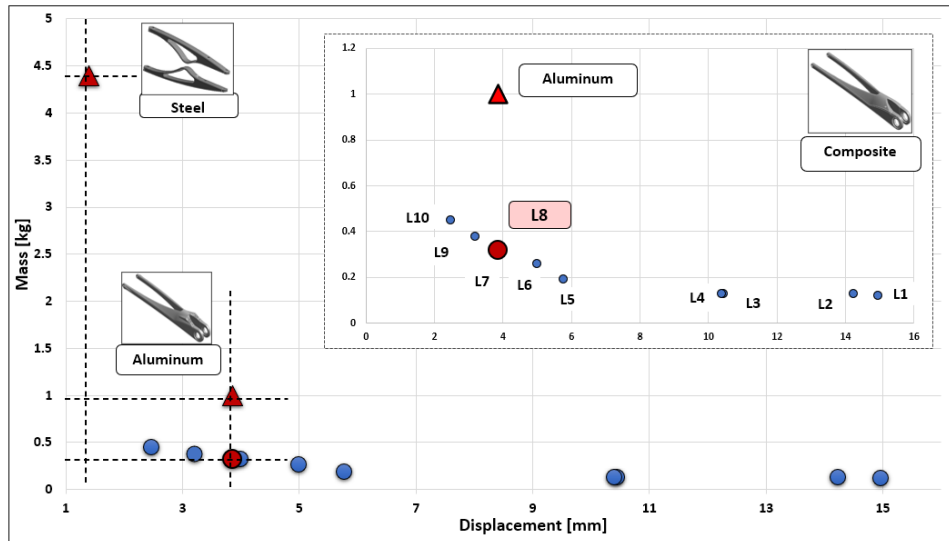
Fig. 5 Effect of stacking sequences on mass and displacement

The *L8* layout, with 14 layers (8 UD) was finally preferred (Tab. 5), able to assure the same stiffness of aluminum (Fig. 6). Beyond the apparent complexity, this layout has thickness of 3.0 mm and a weight of 4.34 g/cm^2, permitting a 3.85 mm displacement with a 0.32 kg of weight. It also exhibits a maximum principal stress in the most stressed layer (2nd layer, in UD) far beyond the tensile stress limit.

UD fabrics were aligned with unidirectional fibers in the same direction, equivalent to the longitudinal direction of the cantilever beam, which also corresponds to the prevailing direction of the lines of forces. Besides, BD fabrics were alternated (0/90 and ±45) to withstand non-prevailing directions of forces. Additional measures such as placing: a) UD close to the surface, away from the neutral plane and b) BD at 0/90 as external protective layers allowed us to improve the results.
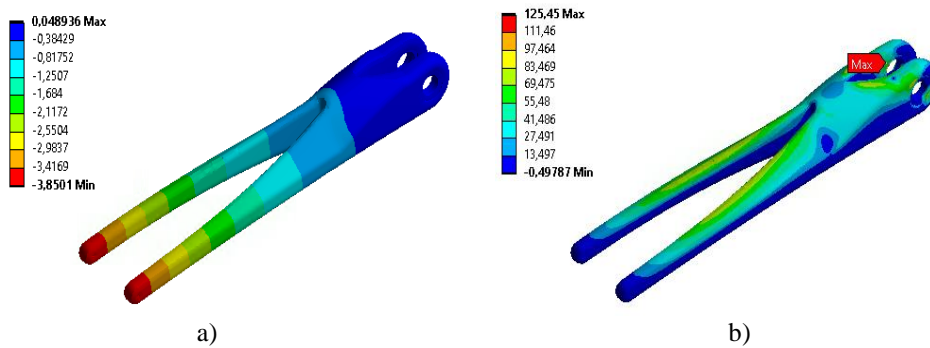

Fig. 6 Mechanic behavior of a fiber-reinforced composite component (Version C) in terms of: a) displacements; b) maximum principal stress (2nd layer)

4.3 Layout Design

During the layout design, different design criteria were introduced noting that:
- UD fabric: a) provides high bending strength against forces aligned with the fibers (0° orientation); b) bends with respect to forces perpendicular to the fibers (90°). In either orientation, it exhibits low torsional strength.
- BD fabric: a) provides medium bending strength and medium torsional strength in a 0° or a 90° orientation; b) is more flexible with high torsional strength at 45°.

As a practical consequence, the layout design followed these practical considerations:
- UD fabrics were used in the presence of and aligned with unidirectional forces.
- BD fabrics were used in the absence of forces along prevailing directions.
- BD fabrics were overlapped, when possible, considering a 45° rotation.

Moreover, composite manufacturing techniques also suggested:
- Layouts were symmetric to avoid differential dilations during cure.
- BD was used for outermost layers.
- Number of layers/cohesive zones between different fabrics was minimized.
- Proper local reinforcements were considered with respect to the most stressed areas.

Table 7 reports the effect of the different stacking sequences on the component in terms of maximum displacement and weight. Their values permit us to better understand the succession of layouts (*L1 - L10*) defined in Table 5 and the redesign process followed.

Table 7 Comparing stiffness and weight of different composite layouts

Layout	L1	L2	L3	L4	L5	L6	L7	L8	L9	L10
Layers	4	6	6	6	10	12	14	14	16	22
Displacement *(mm)*	14.9	14.2	10.4	10.4	5.7	5.0	4.0	3.8	3.2	2.4
Part Weight *(kg)*	0.12	0.13	0.13	0.13	0.19	0.26	0.32	0.32	0.38	0.45

Even if the initial layouts *(L1 - L5)* were not adequate to assure a proper target value of displacement (*i.e.* 3.8 mm), they still permitted to verify, by numerical methods, the effect of: a) using UD instead of BD fabrics; b) fibers orientation.

Useful information emerges, in fact, when layouts were compared by means of displacements:
- *L1* vs. *L2*: displacements are equivalent (14.96 vs. 14.23) even if layouts are different (for equivalent thickness and weight). It depends on the fact that the two layers of used UD, placed orthogonally, are equivalent to a layer of used BD.
- *L3* vs. *L2:* when the fiber orientation is not aligned with the lines of force (*L2*), the displacement increases by 40%. It highlights the positive effect of a proper UD orientation.
- *L3* vs. *L5:* doubling UD layers, the displacement is reduced by a further 45%. It confirms the relevance of a proper UD alignment as criterion for design.
- *L3* vs. *L4:* an insignificant difference emerges with changing the BD orientation. It means the BD direction can be (almost) freely defined. In this regard, it should be noted that the BD layouts have to also consider the risk of unexpected forces.

Although none of these layouts satisfy the target, it is also evident that 8 layers of UD *(L5)* allow to get quite close (5.7 vs. 3.8 mm). The next layouts *(L6-10),* with more layers,

get the target. They were defined also considering the opportunity of: a) not exceeding 4 overlapping layers of the same kind; b) alternating the orientation of the BD layers.

In particular:

- *L6* represents a specular doubling of L3 layout, moving from 6 to 12 layers. The effect is to halve the displacement (5.0 mm).
- *L7* and *L8* add two BD layers to *L6*, on the neutral line, reducing displacement by further 20%. Between the two, the best is *L8* which alternates directions of BDs: with 14 layers, *L8* achieves the target value for displacement (3.8 mm)
- *L9* and *L10* are layouts in which attempts are made to lower displacement (3.20 and 2.47 mm) by adding, respectively, BD or UD to *L8*.

4.4 Failure criteria

Every failure criterion has to consider both the material anisotropy and the specific stacking sequence. In these terms, Fig. 7 shows the Maximum Principal Stress for the most representative layers. In particular, Visible is the 1st layer, in BD (0/90), and the 2nd, in UD. The additional UD layers (3rd – 5th) are not reported since their behavior largely reflects the 2nd with lower stress values. The following BD layers, the 6th at ±45 and 7th at 0/90, are shown. The layers in the lower part are not reported since their behavior symmetrically reflects the upper layers with lower values of stress.
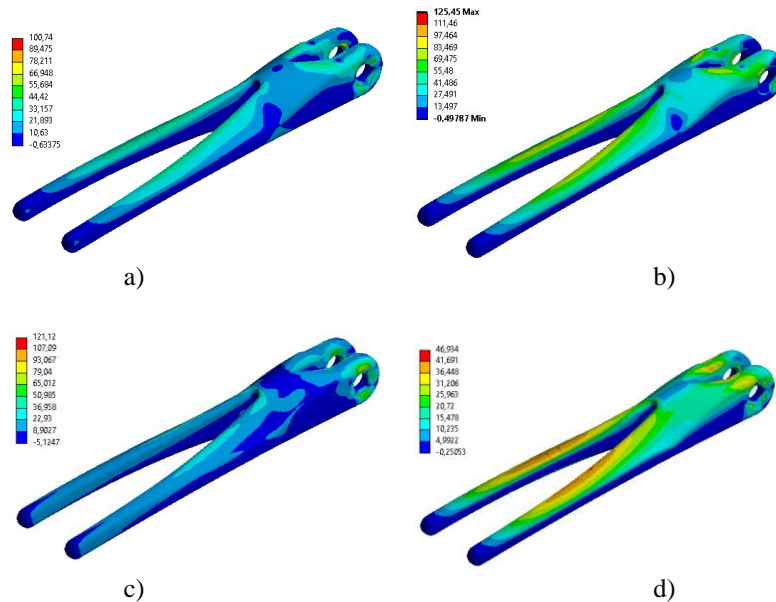

Fig. 7 Maximum Principal Stress for the most relevant layers: a) 1st, BD 0/90; b) 2nd UD 0; c) 6th BD ±45; d) 7th BD 0/90

Specifically, the failures were verified by the application of Maximum Principal Stress and Maximum Distortion Energy (Tsai-Hill) failure criteria in terms of Inverse Reverse Factor (IRF), wherever <<1. The IRF is one parameter commonly used in investigating

the composite failure. The failure load can be defined as the load value divided by IRF. Thus when IRF>1 the composite fails and if IRF<1 it is safe. This is immediately evident in Fig. 8 where, layer by layer, a visual reference with respect to the existing gap between the maximum principal stress and material strength (*i.e.* UTS) is offered.
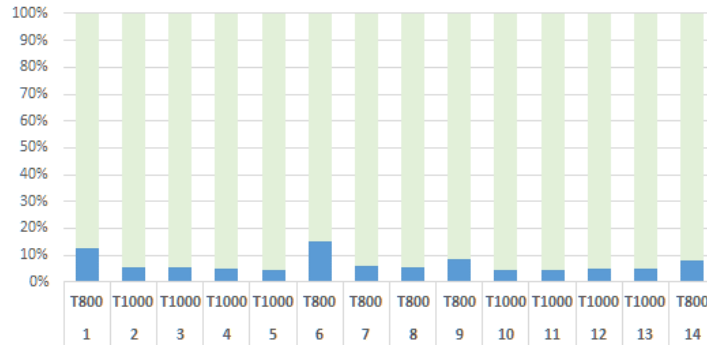

Fig. 8 Layer-by-layer stress and material strength comparison in terms of Inverse Reverse Factor (IRF) and Maximum Principal Stress

To avoid unnecessary bulky structure IRF is normally maintained between 0.5 and 0.75. As a result, this layout may appear oversized. This consideration is correct as long as the present load configuration is taken into account. During the normal use, dissimilar loads can emerge (*e.g.*, misaligned or dynamic) moving away from an ideal condition.

In Fig. 9 failure results with respect to the Tsai-Hill criterion were also reported in terms of Margin of Safety (equal to the inverse of IRF) and considering a load intensification factor of 300%. Not even in this extreme case (*i.e.* a 3-times higher applied load), any criticality emerges except close to the joint where UD layers (especially the 2nd) seem ready to fail (Fig. 9b). This situation is related to the fact that in this zone UD fibers are not always aligned with the lines of force. Thus, UD is found to react along directions where it exhibits a very low stiffness (E = 8600 MPa) and strength (UTS = 29 MPa).
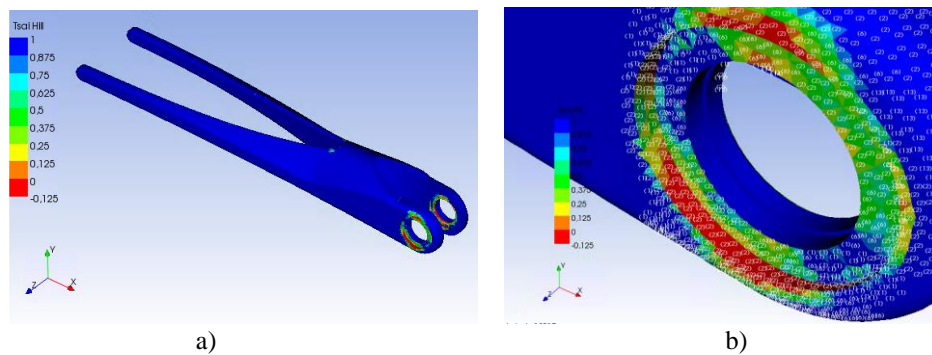

a)   b)

Fig. 9 Margin of Safety with respect to the Tsai-Hill criterion, also reporting the most critical layers

This design challenge, unknown in advance, was solved by:

- strengthening the whole connecting area by substituting UD with BD. Specifically, replacing the same number of layers (*i.e.* 8) three benefits were locally achieved, increasing thickness (from 3.8 to 5 mm), stiffness (from 8600 to 61340 MPa) and strength (from 29 to 805 MPa) with marginal changes in weight (from 0.32 to 0.33 kg).
- inserting a bronze bushing, necessary for the part's correct coupling with the rest of the equipment.

4.5 Prototyping

The component (the forearm) was manufactured in two (asymmetrical) parts, by hand lay-up of prepregs on open molds. Two aluminum molds were made by CNC machining (Fig. 10a). Vacuum bags, with breather assemblies, were placed over the layup and attached to the tool; then a vacuum is pulled prior to initiation of cure. This vacuum bagging process consolidated the plies and reduced voids due to the off-gassing that occurred as the matrix progressed through its chemical curing stages. The cure was performed in autoclave where pressure (6 bar) and temperature (135 °C) facilitated a high fiber volume fraction and low void content for maximum structural efficiency. Additional details on the manufacturing are also available in [25] where a similar process was used.

Then, the parts were extracted from the molds (Fig. 10b), finished (Fig. 10c) and glued. Special inserts, also in CFRP, allowed us to improve the connection.
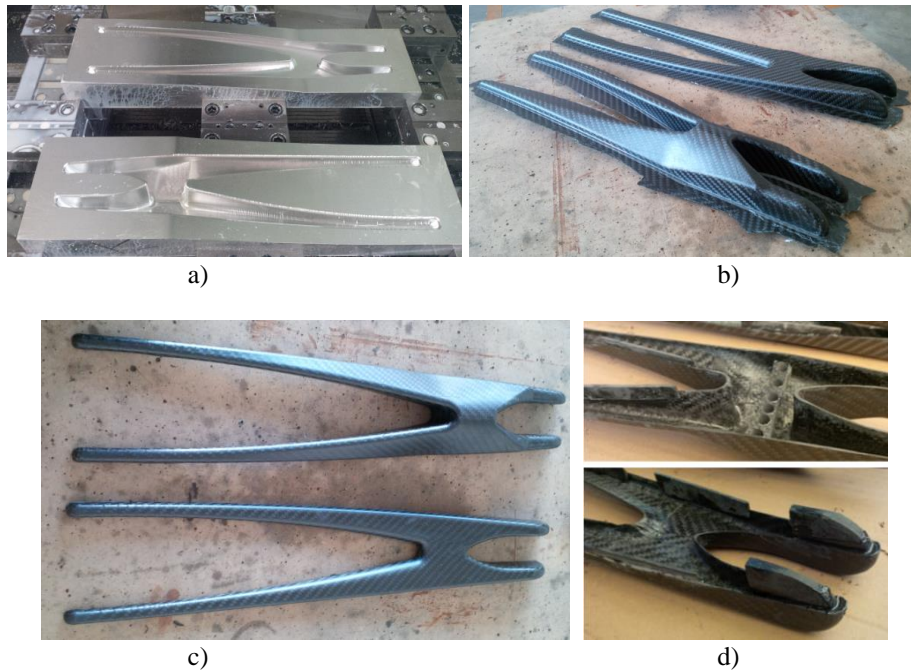

a)   b)

c)   d)

Fig. 10 Production stages: a) molds; b) after curing; c) two sections; d) joining inserts

4.6 The exoskeleton

The design study was extended to the other parts of the upper limb. With respect to the two additional segments, the essential elements of the analysis remain the same. However, as far as possible, the different conditions expected by the statics of the human body were taken into account. For example, the masses of the different body parts were included; the effect of not orthogonal elements (*i.e.* arm and forearm are free to rotate between 0 and 142 degree) were considered. This material change permitted to reduce the segments weight from an initial 17 kg (in the case of aluminum) to the current 8.5 kg (with composites). These segments now include *arm*, *forearm, hand,* and *handle,* for both sides (right and left), and also integrate the resistive elements and the console box.

With respect to the initial design, the jacket (allowing wearing the exoskeleton) and the trapezoids (simulating the shoulders' movement) must be completely redesigned for functional scopes. It is evident that many of their original parts lose functionality in the presence of an exoskeleton. The new target weight is 18kg.

According to [21], where human strength and handling capacity are also classified, in fact, this value is maximum individual weight that can be associated with a "portable" item. However, the same standard, established for military use, also recognizes a weight of 18.5 kg for trained soldiers in operational conditions and 27.7 kilograms when marching. The expected weight reduction will certainly permit going below this higher threshold, making the base not strictly necessary during gym workout.

A support structure, as an option, is still useful to make this new equipment also accessible to the beginner athletes or for different applications (*e.g.* physiotherapy).

5. CONCLUSIONS

A redesign procedure, based on a metal replacement action, is here detailed with the scope to transform advanced gym equipment into a wearable exoskeleton. A first prototype, was designed, produced, and used as gym workout machine. In terms of training functionality, it was fully validated, permitting new and more complex exercises. However, made in steel sheets and aluminum castings, the weight of its moving parts (>48 kg), acting as inertial masses against free athletes' movements, made its utilization rather challenging except for professional trainers. Furthermore, the excessive weight required a bulky support structure, making the whole machine impractical.

The redesign involved the entire upper limb involving changes in shapes, materials, and production processes. Regarding the materials, carbon fiber-reinforced composites were chosen with high-strength fibers (230 GPa) used through epoxy unidirectional and bidirectional fabrics. The effect of fiber properties (as strength and volume ratio) and plies stacking sequences (as thicknesses and orientation) were numerically investigated and a specific layout design was carried out taking into account the direction of forces. External loads higher than expected were considered with an analysis limited to static load configurations.

The narrative is limited to one element of the limb, the forearm, but then extends the results to the entire kinematic chain. For the forearm, it was possible to estimate a weight reduction from 4.4 kg for steel and 1.0 kg for aluminum, to the definitive 0.3 kg in the case of reinforced composites. This result was obtained thanks to a stratification of 14

plies which, however, had a thickness of (only) 3.0 mm and a weight of 4.34 g/m^2 (about half of an aluminum sheet with similar thickness). The structural resistance was verified with the failure criteria provided for anisotropic materials (Maximum Principal Stress, Tsai-Hill) highlighting a Margin of Safety never lower than 25-30%. This margin would allow a further reduction in the stratification. However, the design procedure was addressed to optimize the weight inside the condition to guarantee the same stiffness (compared to solid aluminum). This result was achieved with a 2.85 mm of displacement for a beam of 400 mm subject to a weight of 70 kg. Moreover, additional design steps can lead to the full exploitation of the properties of these high performing composites. In this regard, in fact, before part manufacturing, further design measures were introduced such as: the use of bidirectional composites wherever no prevailing directions of forces emerged; a layout reduction where stress levels were extraordinarily low (*i.e.* side surfaces); addition of reinforcement elements and connection inserts. The part was manufactured by hand lay-up and autoclave curing, confirming the estimated weight reduction of 68% (with respect to aluminum).

This redesign practice was extended to the rest of the entire upper limb, halving the section weight, eliminating the need for support frame, and moving in the direction to transform the original equipment into an active exoskeleton.

REFERENCES

1. Crawford, R.J., Martin, P.J., 2020, *Plastics engineering*, Butterworth-Heinemann.
2. Lyu, M.Y., Choi, T.G., 2015, *Research trends in polymer materials for use in lightweight vehicles*, International journal of precision engineering and manufacturing, 161, pp. 213-220.
3. Han, S.R., Park, J.I., Cho, J.R, 2018, *Development of plastic passenger air bag PAB housing for replacing the steel PAB housing and reducing the automobile weight*, Journal of the Brazilian Society of Mechanical Sciences and Engineering, 404, 224.
4. Kerns, J., 2016, *Replacing metal with plastic*, Machine Design, 88(9), pp. 34-42.
5. Rama, G., Marinkovic, D., Zehn, M., 2018, *High performance 3-node shell element for linear and geometrically nonlinear analysis of composite laminates*, Composites Part B, 151, pp. 118-126.
6. Manalo, A., Aravinthan, T., Karunasena, W., Ticoalu, A., 2010, *A review of alternative materials for replacing existing timber sleepers*, Composite Structures, 923, pp. 603-611.
7. Bai, J., 2013, *Advanced Fibre-Reinforced Polymer (FRP) Composites for Structural Applications - 1st Edition*, Woodhead Publishing.
8. Gürdal, Z., Haftka, R.T., Hajela, P., 1999, *Design and optimization of laminated composite materials*, John Wiley Sons.
9. Almeida, F.S., Awruch, A.M., 2009, *Design optimization of composite laminated structures using genetic algorithms and finite element analysis*, Composite Structures, 883, pp. 443-454.
10. Vukobratovic, M.K., 2007, *When were active exoskeletons actually born?*, International Journal of Humanoid Robotics, 403, pp. 459-486.
11. Hecht, J, 1986, *Armour-suited warriors of the future*, New Scientist, Iss.1527, pp. 31-32.
12. Näf, M.B., Koopman, A.S., Baltrusch, S., Rodriguez-Guerrero, C., Vanderborght, B., Lefeber, D., 2018, *Passive back support exoskeleton improves range of motion using flexible beams*, Frontiers in Robotics and AI, 5, 72.
13. Zoss, A.B., Kazerooni, H., Chu, A., 2006, *Biomechanical design of the Berkeley lower extremity exoskeleton BLEEX*, IEEE/ASME Transactions on mechatronics, 112, pp. 128-138.

14. Veneman, J.F., Kruidhof, R., Hekman, E.E., Ekkelenkamp, R., Van Asseldonk, E.H., Van Der Kooij, H. 2007, *Design and evaluation of the LOPES exoskeleton robot for interactive gait rehabilitation*, IEEE Transactions on Neural Systems and Rehabilitation Engineering, 153, pp. 379-386.

15. Perry, J.C., Rosen, J., Burns, S., 2007, *Upper-limb powered exoskeleton design*, IEEE/ASME Transactions on Mechatronics, 124, pp. 408-417.

16. Wang, J., Li, J., Zhang, Y., Wang, S., 2009, *Design of an exoskeleton for index finger rehabilitation*, IEEE Engineering in Medicine and Biology Society, pp. 5957-5960.

17. Perry, J., Rosen, J., 2008, *EXOSKELETON*. U.S. Patent Application No. 11/729, 998.

18. Fragassa, C., Berardi, L, Balsamini, G., 2016, *Magnetorheological fluid devices: an advanced solution for an active control on the wood manufacturing process*, FME Transactions, 44(4), pp. 333-339.

19. DOD, U., 1994, *Military Handbook: Metallic Materials and Elements for Aerospace Vehicle Structures*, MIL-HDBK-5G, 2 vols. US Department of Defense, Wright-Patterson AFB, OH, USA.

20. Toray: Type of Composite Fibers, https://www.toraycma.com/page.php?id=661. (access on 20.03.2020).

21. DoD, M.S., 2012, *Design Criteria Standard: Human Engineering (MIL-STD-1472g). (Section 5.8.6)*, Department of Defense, Washington.

22. Zienkiewicz, O. C., 1977, *The Finite Element Method. 3. Edition*, London. McGraw- Hill Book Company (UK) Limited. XV, 787p.

23. Bogenfeld, R., Kreikemeier, J., Wille, T., 2018, *Review and benchmark study on the analysis of low-velocity impact on composite laminates*, Engineering Failure Analysis, 86, pp. 72-99.

24. Rajbhandari, S.P., Scott, M.L.; Thomson, R.S., Hachenberg, D., *An approach to modelling and predicting impact damage in composite structures*, In Proceedings of the ICAS Congress, Toronto, ON, Canada, 8th-13th, September 2002, pp. 8-13.

25. Fragassa, C., 2017, *Marine Applications of Natural Fibre-Reinforced Composites: A Manufacturing Case Study*, In: Pellicer E. et al. (Eds.), *Advances in Application of Industrial Biomaterials*, Springer International Publishing, Cham, CH, doi: 10.1007/978-3-319-62767-0_2, pp. 21-47.